Climate Dynamics (2006)
DOI 10.1007/s00382-006-0129-5

Timothy J. Osborn · Sarah C. B. Raper
Keith R. Briffa

Simulated climate change during the last 1,000 years: comparing the ECHO-G general circulation model with the MAGICC simple climate model

Received: 24 May 2005 / Accepted: 19 January 2006

Abstract An intercomparison of eight climate simulations, each driven with estimated natural and anthropogenic forcings for the last millennium, indicates that the so-called "Erik" simulation of the ECHO-G coupled ocean-atmosphere climate model exhibits atypical behaviour. The ECHO-G simulation has a much stronger cooling trend from 1000 to 1700 and a higher rate of warming since 1800 than the other simulations, with the result that the overall amplitude of millennial-scale temperature variations in the ECHO-G simulation is much greater than in the other models. The MAGICC (Model for the Assessment of Greenhouse-gas-Induced Climate Change) simple climate model is used to investigate possible causes of this atypical behaviour. It is shown that disequilibrium in the initial conditions probably contributes spuriously to the cooling trend in the early centuries of the simulation, and that the omission of tropospheric sulphate aerosol forcing is the likely explanation for the anomalously large recent warming. The simple climate model results are used to adjust the ECHO-G Erik simulation to mitigate these effects, which brings the simulation into better agreement with the other seven models considered here and greatly reduces the overall range of temperature variations during the last millennium simulated by ECHO-G. Smaller inter-model differences remain which can probably be explained by a combination of the particular forcing histories and model sensitivities of each experiment. These have not been investigated here, though we have diagnosed the effective climate sensitivity of ECHO-G to be 2.39 ± 0.11 K for a doubling of CO_2.

T. J. Osborn (✉) · S. C. B. Raper · K. R. Briffa
Climatic Research Unit, School of Environmental Sciences,
University of East Anglia, Norwich NR4 7TJ, UK
E-mail: t.osborn@uea.ac.uk
Tel.: +44-1603-592089
Fax: +44-1603-507784

S. C. B. Raper
Dalton Research Institute,
Manchester Metropolitan University, Manchester, UK

1 Introduction

The MAGICC (Model for the Assessment of Greenhouse-gas-Induced Climate Change) simple climate model (Wigley and Raper 1992, 2002) comprises a surface energy-balance coupled with a one-dimensional ocean column model that parameterises vertical heat transport processes by a combination of advection (upwelling) and diffusion. The only horizontal resolution is provided by the separate representation of the land and ocean areas within each hemisphere (a total of four boxes). Nevertheless, with appropriate choices (i.e. tuning) for its various parameters, the MAGICC model is able to closely replicate the hemispheric- and global-scale response to rapidly increasing greenhouse gases simulated by much more complex general circulation models (GCMs) (e.g. Fig. 6.17 of Kattenberg et al. 1996; Raper and Cubasch 1996; Raper et al. 2001). MAGICC has been used extensively for generating future climate change scenarios, because of its ability to replicate some GCM behaviour with just a few tunable parameters which then allows it to be run quickly under a range of radiative forcing scenarios for which the GCM has not been run (Kattenberg et al. 1996; Cubasch et al. 2001; Wigley and Raper 2002). It is also easy to explore the dependence of climate response on the model's parameter space (Wigley and Raper 2001). Other simple climate models have been used for similar purposes (Harvey et al. 1997; Kheshgi and Jain 2003; Yohe et al. 2004).

Simple climate models, including MAGICC, have also been used to simulate the response to the smaller radiative forcing changes that are likely to have occurred during recent centuries and the last millennium (e.g. Free and Robock 1999; Crowley 2000; Crowley et al. 2003; Foukal et al. 2004). Similar simulations have also been

undertaken with intermediate complexity and GCM-based climate models (Bertrand et al. 2002; Bauer et al. 2003; Gerber et al. 2003; von Storch et al. 2004; S.F.B. Tett et al., submitted for publication; C.M. Ammann et al., submitted for publication). One such GCM-based experiment is the "Erik" simulation, run for the last 1,000 years with the ECHO-G model (von Storch et al. 2004; also see Sect. 2). A visual comparison of these simulations (see Sect. 3) suggests that the "Erik" simulation exhibits quite different behaviour than the other experiments, with greater multi-centennial Northern Hemisphere (NH) temperature variations. The purpose of the present paper is to demonstrate that the MAGICC model, with appropriate tuning, can closely reproduce the ECHO-G Erik simulation at global and hemispheric scales, and can be used to investigate possible reasons for the atypical behaviour of the Erik simulation.

Exploring how well the MAGICC model is able to replicate the behaviour of the ECHO-G Erik simulation over this period is a valuable test in itself, given that most previous comparisons have focussed on future changes when the forcing change is usually of one sign (increasing) and where the time scale of the response is determined to a large extent by the time scale of the strongly increasing forcing. Within the past 1,000 years, the climate forcing (Sect. 2) both increased and decreased over time, and the structure of the forcing variability places emphasis on the ability of MAGICC to simulate the approach to new climate equilibria, as well as the more immediate response to a transient forcing change. The climate sensitivity is diagnosed from the ECHO-G Erik simulation (Sect. 4) and is then used in the MAGICC model, together with tuning of its other parameters (Sect. 5), to attempt to replicate the Erik simulation. Having achieved at least partial success, the tuned MAGICC model is then used to investigate possible explanations for the atypical behaviour of the ECHO-G Erik simulation compared with other simulations of the last 1,000 years. The factors considered here are the disequilibrium in the initial conditions of the experiment and the absence of any negative forcing during the 20th century from tropospheric sulphate aerosols (Sect. 6). The importance of these factors in explaining the different behaviour is then evaluated in Sect. 7 by returning to the comparison with other model simulations. Finally, the results are discussed and summarised in Sect. 8. A related study (Goosse et al. 2005) was published just as the present study was completed; the implications of the results obtained here for the conclusions of Goosse et al. (2005) are also discussed in Sect. 8.

2 Description of the ECHO-G model and the Erik simulation

The ECHO-G climate model (Legutke and Voss 1999) consists of the ECHAM4 atmospheric GCM coupled to the HOPE-G ocean GCM, both developed at the Max-Planck-Institute for Meteorology in Hamburg. The simulations used here were undertaken by the Institute for Coastal Research at GKSS in Germany and the Universidad Complutense de Madrid in Spain. The configuration used for the Erik simulation (so-called because of the similarity between its start date and the settlement of Greenland by Erik the Red) has 19 vertical levels in the atmosphere and 20 in the ocean, and horizontal resolutions of approximately 3.75° (atmosphere) and 2.8° (ocean) in both latitude and longitude (the oceanic meridional resolution is enhanced in the tropical regions, reaching 0.5° at the equator). To enable the coupled model to sustain a simulated climate near to the real present-day climate, with minimal drift, the heat and freshwater fluxes between atmosphere and ocean are modified by constant (in time) fields of adjustment terms.

A 1,000-year control simulation (Zorita et al. 2003) was generated using fixed external forcings set to present-day values (solar constant = 1,365 W m^{-2}; $[CO_2]$ = 353 ppm; $[CH_4]$ = 1,720 ppb; $[N_2O]$ = 310 ppb). The flux adjustments were successful in preventing a long-term drift in the global-mean 2 m air temperature, though regional changes do occur with warming in the Southern Hemisphere (SH) and cooling in the NH of the order 0.2 K over the 1,000-year run (see Sect. 6 for further details about model drift).

The "Erik" simulation (Gonzalez-Rouco et al. 2003; von Storch et al. 2004) is an attempt to model climate variations from 1000 to 1990, as a response to natural and anthropogenic forcings. The following forcings were included as input to the ECHO-G model: (i) combined anthropogenic and natural fluctuations in the concentrations of the CO_2, CH_4 and N_2O well-mixed greenhouse gases (including pre-industrial fluctuations in CO_2 and CH_4); (ii) natural variations in solar irradiance generated by Crowley (2000) from a combination of the Lean et al. (1995) sunspot-based estimates and an ice core record of the cosmogenic isotope ^{10}Be, but with greater magnitude than the Crowley (2000) series due to the scaling that Gonzalez-Rouco et al. (2003) applied to match its variance to that of the Lean et al. (1995) time series during the 20th century (von Storch et al. 2004, supplementary information); and (iii) natural variations in volcanic aerosols, parameterised as reductions in solar irradiance, according to Crowley (2000). A number of potentially important forcings were not included in the Erik experiment, most notably the negative forcing due to anthropogenic tropospheric sulphate aerosols during the 20th century, but also variations in some other greenhouse gases (halocarbons and ozone) and the effect of land-use changes.

The initial conditions of the Erik simulation were taken from year 100 of the control run. Those initial conditions are, however, representative of present-day rather than pre-industrial climate and the experimental design therefore included a 30-year adjustment period during which the control run forcing was linearly reduced until it matched the forcing appropriate for AD 1000, followed by a 50-year period with fixed

forcing to allow the model's climate to respond to the reduced forcing (solar constant = 1,364.92 W m^{-2}; $[CO_2] = 283$ ppm; $[CH_4] = 691$ ppb; $[N_2O] = 277$ ppb). The Erik simulation then proceeded from the conditions at the end of this latter period. The possibility of continuing adjustment, after the start of the Erik simulation, to this initial reduction in radiative forcing is considered in Sect. 6. The total of all forcing factors is shown in Fig. 1, including the pre-1000 adjustment period (the calculation of this total forcing is described in Sect. 4).

3 Comparison of the Erik simulation with other simulations

Figure 2a presents an intercomparison of a number of published climate simulations that span at least the last 1,000 years (the HadCM3 simulation for 1500–1999 is also included). These are based on energy-balance, intermediate complexity and GCM-based climate models (references are given in the caption), including the Erik simulation with ECHO-G. The inter-model spread of simulated temperatures is not solely attributable to different model behaviour because the initial conditions and radiative forcings differ between each simulation. The simulated parameter shown is the annual NH mean temperature, smoothed and expressed as anomalies from the 1901–1960 reference period. Mean NH temperature was selected because it is more frequently compared with palaeoclimate reconstructions than other regions/variables, due to the difficulty in reconstructing past temperatures in the SH from the existing sparse climate proxy records (Mann and Jones 2003). A similar impression is, however, obtained from an intercomparison of the global-mean temperatures of these simulations (not shown).

The various model simulations exhibit significant spread away from the 1901–1960 reference period, with much of the "divergence" of individual simulations occurring between 1700 and 1900. Prior to 1700 the simulations approximately parallel each other, with the exception of the ECHO-G Erik simulation. This model run is the coolest out of all runs between 1520 and 1850, yet is one of the warmest between 1000 and 1150. The reference period used in Fig. 2a tends to direct the focus towards differences in the relative coolness of the "Little Ice Age" period, and hence also on explanations for differences in this coolness such as model sensitivity or the particular forcings applied [e.g. Mann et al. (2005) argue that the solar forcing used in this experiment is unusually large, though intercomparison of the solar forcing histories applied in each of the simulations in Fig. 2 indicates that the magnitude of forcing differences is relatively small].

A rather different visual impression is given by a change to the reference period. Figure 2b shows the same NH temperature simulations, but now expressed as anomalies from the 1500–1899 period. Each curve in Fig. 2b is simply shifted vertically from its position in Fig. 2a, by an amount equal to the difference between the 1901–1960 and 1500–1899 means for each series. In Fig. 2b, the ECHO-G Erik simulation clearly stands out as having different behaviour to the other model runs, with a much warmer pre-1250 period and also considerably greater warming during the final two centuries. Investigation of the possible causes for this atypical behaviour, using the MAGICC simple climate model, is the focus of the remainder of this paper.

4 Diagnosing the mean effective climate sensitivity and reference temperature for Erik

Most of the MAGICC model parameters do not have a direct physical counterpart with a parameter or diagnostic of the ECHO-G model (e.g. although the HOPE ocean GCM uses a specific value for vertical thermal diffusivity, this value would not be appropriate for the MAGICC vertical diffusivity because in MAGICC that term is used to represent a whole range of heat penetration processes, not just diffusion). Appropriate values of some parameters can be diagnosed from GCM simulated data [Raper et al. (2001) do in fact attempt to

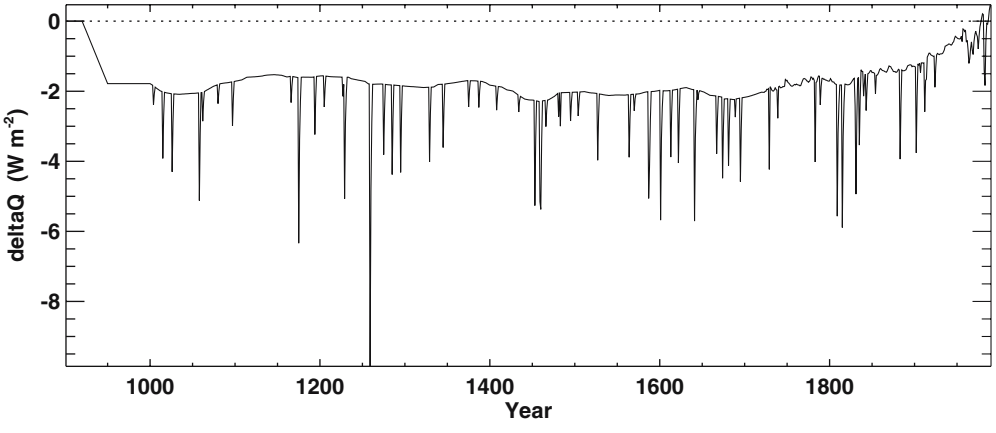

Fig. 1 History of radiative forcing (W m^{-2}) used during the ECHO-G Erik simulation, including the pre-1000 spin-up period. The forcing combines solar, volcanic and greenhouse gas variations. Values are expressed as anomalies from the forcing used in the ECHO-G present-day control run, marked by the *dotted line*

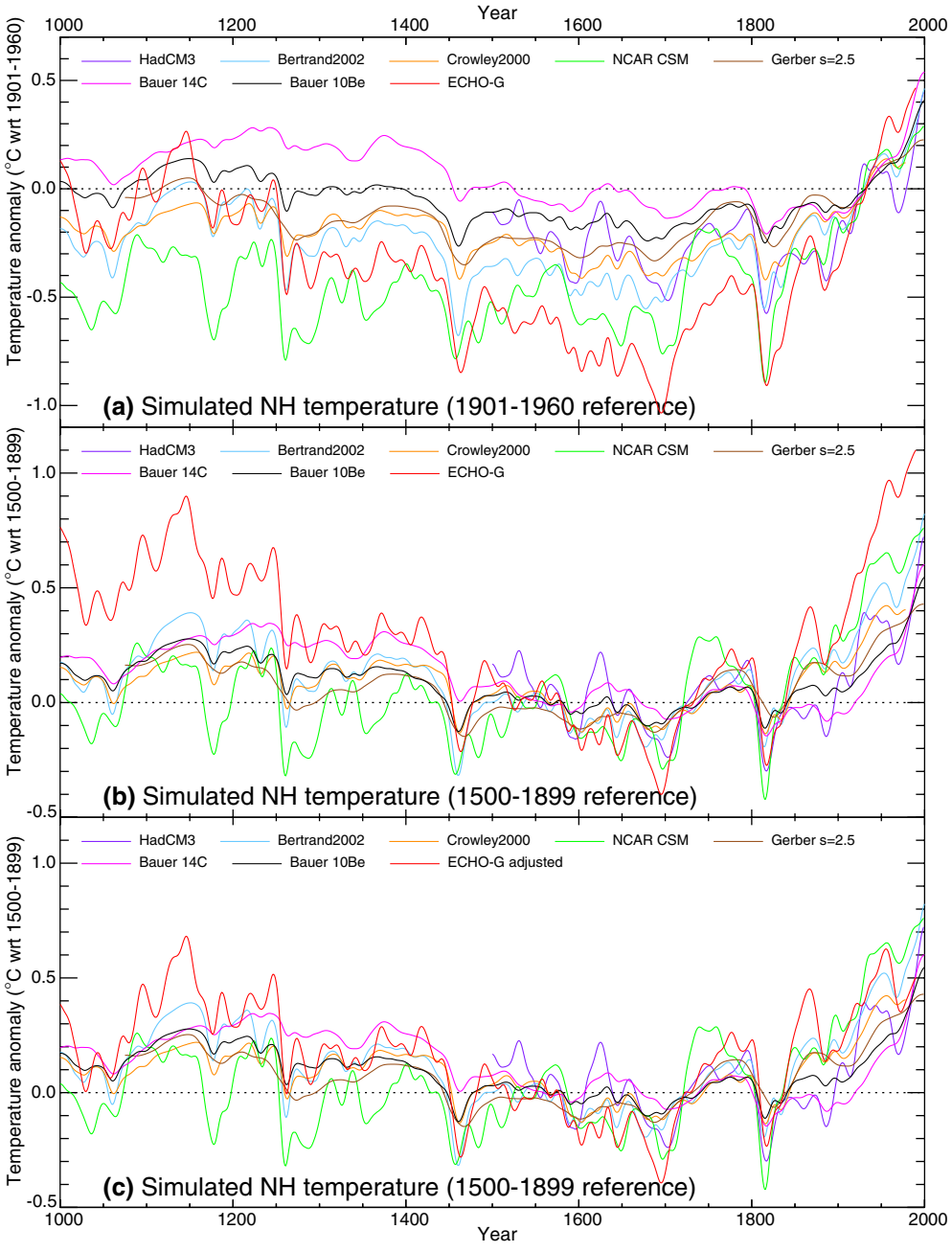

Fig. 2 Comparison of Northern Hemisphere mean temperature time series simulated by energy-balance models (*orange*: Crowley 2000); intermediate complexity models (*blue*: Bertrand et al. 2002; *pink* and *black*: Bauer et al. 2003 with solar irradiance changes estimated using ^{14}C and ^{10}Be records, respectively; *brown*: Gerber et al. 2003, with a climate sensitivity of 2.5 K for CO_2 doubling); and general circulation model-based climate models (*red*: ECHO-G, Gonzalez-Rouco et al. 2003; *green*: NCAR CSM, C.M. Ammann et al., submitted for publication; *purple*: HadCM3, Widmann and Tett 2003; S.F.B. Tett et al., submitted for publication). Each series is expressed as anomalies from its mean calculated over **a** 1901–1960; and **b** and **c** 1500–1899; and smoothed with a 30-year filter. In (**c**), the *red* ECHO-G line is adjusted according to the estimates of early climate drift and recent sulphate aerosol cooling obtained in this paper

diagnose appropriate values of ocean vertical diffusivity from a simulation with the HadCM2 climate model], but in most cases it is simpler (and requires less GCM data) to estimate parameter values by trial and error. One exception is the climate sensitivity, which can be diagnosed directly from the GCM simulation.

The global-mean surface energy-balance can be approximated by

$$\Delta Q = \lambda \Delta T + F \qquad (1)$$

which simply requires that any anomalous radiative forcing (ΔQ) that is applied to the model is balanced by the rate of climate system heat content change (F) and a perturbation to the long-wave radiative heat loss to space, that is itself a linear function of the surface temperature anomaly (ΔT). The coefficient λ, which relates long-wave radiation change to the surface temperature anomaly, is inversely proportional to the climate sensitivity: $s = 1/\lambda$, where the units of s are K/(W m^{-2}). If the system reaches a new equilibrium, $F = 0$ and $\Delta T = s\,\Delta Q$. If the forcing applied to the model is equivalent to that generated by a doubling of the CO_2 concentration [$\Delta Q_{2\times CO_2} = 3.71$ W m^{-2} is the estimate given by Ramaswamy et al. (2001)], then $\Delta T_{2\times CO_2} = s\Delta Q_{2\times CO_2}$ is the familiar climate sensitivity expressed as the equilibrium warming expected following a doubling of CO_2. Equa-

tion 1 is commonly applied to estimate the climate sensitivity from equilibrium simulations ($F=0$) with GCMs. However, Eq. 1 is also applicable to transient model runs, using GCM-simulated values for ΔQ, ΔT and F to estimate what is often called the "effective" climate sensitivity of the model (Murphy 1995; Raper et al. 2001).

Appropriate values of ΔQ are not straightforward to calculate from GCMs, however, because they are usually taken to represent forcing at the top of the troposphere and thus need to be adjusted for any changes in the stratospheric temperature (Hansen et al. 1997). Gregory et al. (2004) demonstrate how Eq. 1 can be used to estimate both the climate sensitivity and ΔQ from a transient GCM simulation, provided that ΔQ is constant during the simulation (i.e. a step-function change in forcing, which is then maintained for the length of the simulation). The Gregory et al. (2004) method cannot be used here because the forcing is not constant during the ECHO-G Erik simulation; therefore the forcing was estimated directly from the inputs prescribed to the model. The forcing due to variations in greenhouse gases was estimated using the algorithms given in Table 6.2 of Ramaswamy et al. (2001). This was combined with the known radiative forcing that was applied to the model in the form of a changing effective solar irradiance to represent the combination of the solar and volcanic forcings (see also Sect. 2). The effective solar irradiance was divided by 4 (the ratio of the area of the Earth's surface to the area of the solar flux that the Earth intercepts) and multiplied by the average planetary co-albedo during the simulation. The combined greenhouse gas, solar and volcanic forcing is shown in Fig. 1.

Given this estimated time series of ΔQ (which is likely to be very close to the actual forcing felt by the model), and actual simulated time series of ΔT and F, Eq. 1 can be used to estimate the effective climate sensitivity. Before this calculation can be done, however, appropriate reference levels for ΔQ and ΔT must be obtained (F is an absolute heat gain by the ocean and land surface of the climate system, rather than an anomaly from some reference period). The problem is not as simple as expressing both the forcing and the temperature as anomalies from some reference period mean. This is fine for the forcing, but the temperature would then need to be expressed as anomalies from the *equilibrium* temperature that would have been achieved under the reference period forcing. This is not simply the mean temperature simulated during the reference period, unless the simulated climate was in equilibrium with the forcing at that time. Here, we express the forcing relative to the present-day control run forcing, but the initial conditions in year 900 of the simulation (taken from the ECHO-G present-day control simulation) may not be appropriate to use as a reference temperature because the model may not have been in equilibrium (as indicated by a small long-term drift). Instead, we will independently estimate both the reference temperature and the effective climate sensitivity.

Plotting values of $F - \Delta Q$ against the ΔT values should, according to Eq. 1, give values that lie approximately along a straight line with slope $-\lambda$. The line will also go through the origin if the reference temperature chosen for expressing ΔT was correct; if this was estimated incorrectly, then the regression line fitted to the data will intercept the x-axis at a non-zero value and this non-zero value can be subtracted from the estimated reference temperature to obtain the correct reference temperature. Figure 3 shows such a plot, with the reference temperature adjusted to force the regression line to pass through the origin. It is not clear which variable should be considered as the dependent variable in the regression, because both F and ΔT include random variability (Gregory et al. 2004). The regression has, therefore, been done in both ways and the geometric mean of the two slopes is used [also known as the "line of organic correlation"—Hirsch and Gilroy (1984)]. The results also show some sensitivity to the period of data used for the analysis and the time averaging applied.

Annual-mean values from the full 1000–1990 period show a highly significant correlation of $r=-0.81$ (Fig. 3). For ΔQ expressed as a perturbation from the radiative forcing of the ECHO-G present-day control simulation (Fig. 1), a reference temperature of 287.9 K is obtained (the mean temperature from the ECHO-G present-day control simulation for the years of overlap with the Erik simulation is also 287.9 K). The regression slope yields $s=0.64$ K/(W m^{-2}) (with a 95% uncertainty range of 0.62–0.68), which is equivalent to $\Delta T_{2\times CO_2} =$ 2.39 K (95% range 2.28–2.50). These ranges are calculated using standard formulae for regression parameters and as such are likely to considerably underestimate the true uncertainty because (i) the annual values are

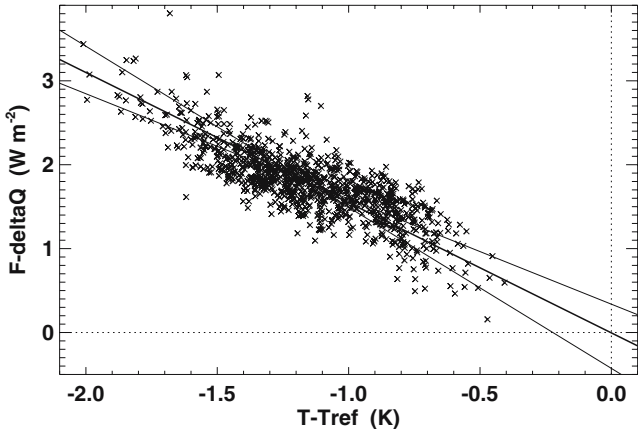

Fig. 3 Annual-mean values of implied long-wave radiative heat loss ($F - \Delta Q$, W m^{-2}, with ΔQ expressed as anomalies from the ECHO-G present-day control run forcing) versus global-mean temperature anomaly (ΔT, K, expressed as anomalies from a reference period that allows the regression line to pass through the origin). The regression line (*thick*) is obtained using the geometric mean of the slopes of the least-squares fits of y on x and x on y, which are also shown (*thin*) as an ad hoc measure of uncertainty

autocorrelated and thus the effective independent sample size is much less than 991 years; (ii) the choice of regression method yields a larger range for $\Delta T_{2\times CO_2}$ (1.93–2.96 K); (iii) longer time averaging yields higher values for $\Delta T_{2\times CO_2}$ (up to 2.99 K for 90-year means).

5 Replicating the Erik simulation using the MAGICC simple climate model

The MAGICC climate model resolves the air temperature over land and ocean separately, which are determined by a radiative energy-balance combined with heat transfers between the land and ocean and between the two hemispheres (the latter occurring only between the ocean boxes of the hemispheres) and ocean heat uptake (the land heat capacity is assumed to be zero). Following Sect. 4, the effective climate sensitivity is prescribed to be $\Delta T_{2\times CO_2} = 2.39$ K. Selection of other parameters is by trial and error to obtain good fits between the global and hemispheric temperatures simulated by MAGICC and ECHO-G under the same forcing and spin-up conditions (with the exception that the initial conditions in year 900 are selected to be in equilibrium with the present-day control run forcing for MAGICC, but may not be in equilibrium for ECHO-G due to ongoing drift in the ECHO-G present-day control run). The final variable that is used to constrain the tuning is the ocean heat uptake time series (i.e. *F*). This is particularly useful, both because it is an absolute value (not an anomaly) and thus provides a more stringent test of the MAGICC model and because it can be used to differentiate between situations where a given temperature change could have occurred either from a high climate sensitivity damped by strong ocean heat uptake, or from a lower climate sensitivity combined with weaker ocean heat uptake.

The tuned parameter values are shown in Table 1 and the match between the MAGICC and ECHO-G simulations is presented in Fig. 4 for long-term changes and in Fig. 5 for the composite response to individual volcanic events. ECHO-G data were not available for the pre-1000 adjustment period. The agreement between the simulations is excellent for most periods, time scales and for the three variables shown. The biggest mismatch is a difference in the multi-century rate of cooling in the first centuries of the simulations, for both the global (Fig. 4a) and NH temperatures (Fig. 4b); it appears that the two simulations gradually converge, and after 1500 they follow each other closely. It proved impossible to tune MAGICC to reproduce the strength of the 1000–1500 cooling, given the prescribed forcing history (Fig. 1) because there is only a small trend in the forcing over that period. The strength of the modern global-mean warming is very slightly larger in the MAGICC results than in ECHO-G (Fig. 4a), but there is a good match for the NH temperature (Fig. 4b). Given that the climate sensitivity should not be altered because it was diagnosed rather than tuned, the only way to reduce the rate of modern global warming would be to increase the heat uptake by the MAGICC ocean (perhaps by further tuning of the ocean mixing parameters or the land–ocean exchange coefficients). That would, however, deteriorate the current excellent match between the MAGICC and ECHO-G ocean heat fluxes (Fig. 4c). Given these constraints, it is probably not possible to achieve much improvement in the already good fit between the models on these long time scales.

Table 1 MAGICC (Model for the Assessment of Greenhouse-gas-Induced Climate Change) model parameters obtained after tuning to replicate the ECHO-G Erik simulation

Parameter	Symbol	Tuned value	Units
Global climate sensitivity	$\Delta T_{2\times CO_2}$	2.39	K
Ratio of land to ocean equilibrium temperature change	*RLO*	1.4	–
Land–ocean exchange coefficient	*LO*	5.0	W m^{-2} K^{-1}
Interhemispheric exchange coefficient	*NS*	0.5	W m^{-2} K^{-1}
Mixed layer depth	*hm*	60.0	m
Ocean vertical diffusivity	*k*	2.3	cm^2 s^{-1}
Present-day upwelling rate	*w*	4.0	m $year^{-1}$
Magnitude of warming that would reduce *w* by 30%[a]	ΔT^+	10.0	K

All other parameters are unchanged from Appendix 9.1 of Cubasch et al. (2001) and Wigley and Raper (2002)
[a]To represent a collapse of the thermohaline circulation (Appendix 9.1 of Cubasch et al. 2001)

The decadal time scale response to volcanic forcing spikes shown in Fig. 4 is also well replicated by MAGICC with only minor differences: the decadal temperature responses are somewhat larger in ECHO-G, while the ocean heat flux responses are slightly weaker. The *shape* of the heat flux response on both multi-decadal (Fig. 4c) and sub-decadal time scales (Fig. 5e, f) is, however, similar in the two models: initial oceanic cooling, followed by heat uptake as the climate recovers to its previous level, with a characteristic exponential-type decay. The initial oceanic heat loss (Fig. 5e, f) in the year of the eruption is too strong in MAGICC for most events and in the composite mean, though the difference is only marginally significant when compared with the sampling variability evident within the composite. The high heat loss during eruption years is due in part to the large land–ocean exchange coefficient selected (*LO* in Table 1), which efficiently transfers heat loss from the land to ocean boxes of the MAGICC model and was necessary to distribute the peak cooling from the year of the eruption (year 0 in Fig. 5) more equally across years 0 and 1 (Fig. 5a–d). With the much lower *LO* values used in previous work (Cubasch et al. 2001; Wigley and Raper 2002), year 0 cooling was much too great in MAGICC due to a very large cooling over the land boxes (which have zero heat capacity in this model and thus respond immediately to the balance between

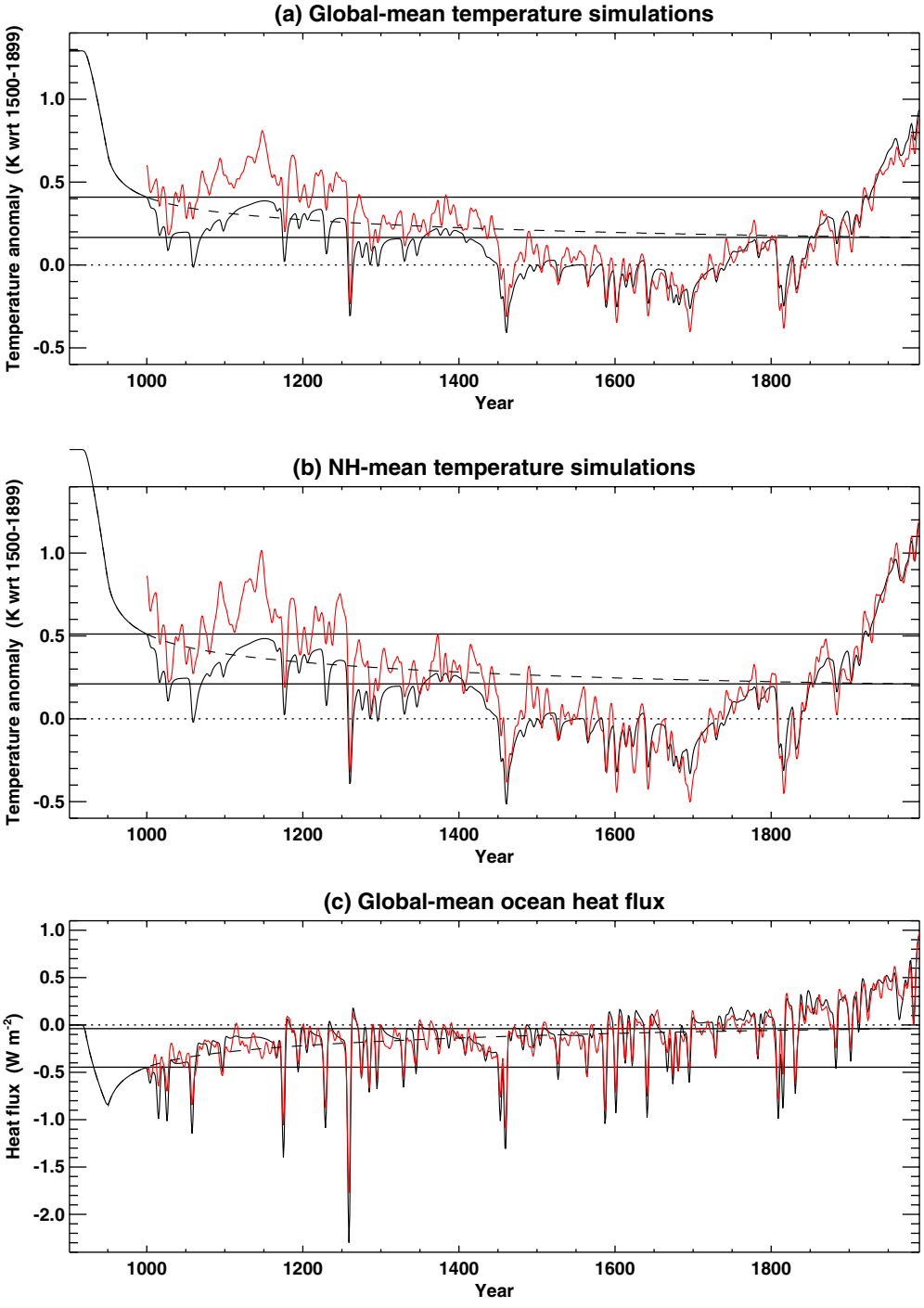

Fig. 4 Time series of **a** global-mean temperature (K), **b** Northern Hemisphere temperature (K) and **c** global-mean heat flux into the ocean (W m^{-2}) as simulated by the ECHO-G general circulation model (*red*) and the MAGICC (Model for the Assessment of Greenhouse-gas-Induced Climate Change) simple climate model (*black*). The temperature series are expressed as anomalies from their 1500–1899 means, while the heat fluxes are in absolute units with fluxes into the ocean positive. Each series is smoothed with a 10-year filter. Also shown (*dashed*) is the MAGICC simulation with radiative forcing held fixed from 1000 onwards, to indicate the ongoing adjustment to the pre-1000 spin-up; the two *horizontal solid lines* mark the climate change in this run between 1000 and 1990

radiation and land–ocean exchanges). Note that a higher land–ocean exchange also reduces the apparent time variation in effective climate sensitivity that can arise due to the different land and ocean response times (Raper 2004). All other differences in the volcanic composites are within the range of sampling variability

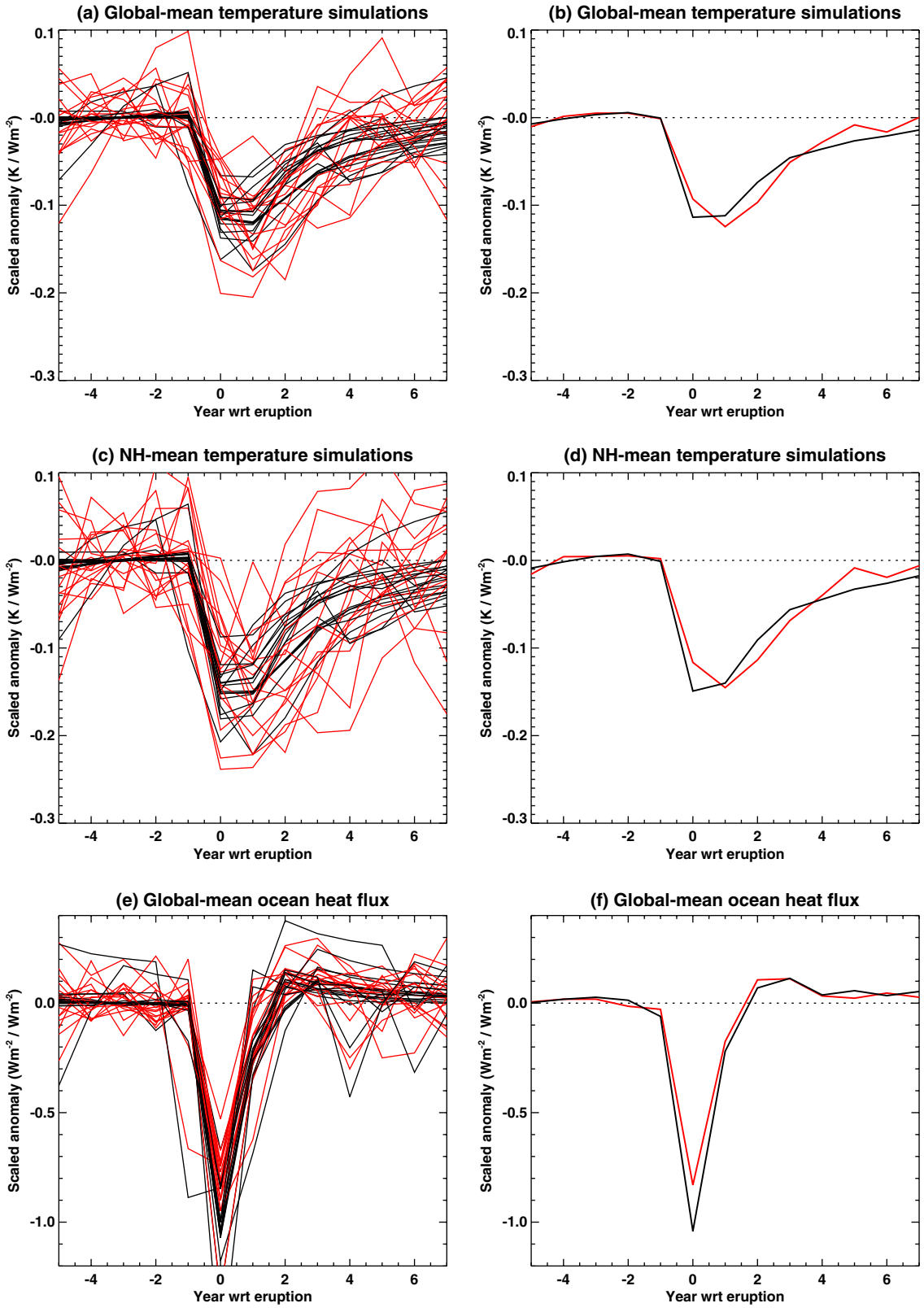

Fig. 5 Composite members (**a**, **c**, **e**) and composite means (**b**, **d**, **f**) of **a** and **b** global-mean temperature (K), **c** and **d** Northern Hemisphere temperature (K) and (**e** and **f**) global-mean heat flux into the ocean (W m^{-2}) as simulated by the ECHO-G general circulation model (*red*) and the MAGICC (Model for the Assessment of Greenhouse-gas-Induced Climate Change) simple climate model (*black*). Composites are selected and aligned according the 17 largest spikes in the volcanic forcing applied to the models, each expressed as anomalies from the mean of the 5 years prior to the peak negative forcing, and then divided (scaled) by magnitude of the peak negative forcing

expected for a composite of this size, and thus the temperature response and subsequent recovery, as well as the ocean heat flux in years 1–7 after the eruption, are well replicated by MAGICC. Similarly good results have also been obtained using MAGICC tuned to fit simulations with the NCAR/US DOE Parallel Climate Model (Wigley et al. 2005), though for that case it was not necessary to use a large land–ocean exchange coefficient.

Though we have focussed in some detail on the intricacies of the MAGICC behaviour, this was to justify the decisions that must be made when tuning such a model, rather than to imply that the relatively minor differences between MAGICC and ECHO-G restrict the potential for our use of MAGICC. The only large difference is in the rate of cooling from 1000 to 1500, and this is considered further in the next section.

6 Using MAGICC to estimate the impact of initial climate adjustment and best-guess tropospheric sulphate aerosols on the Erik simulation

It seems likely that climate drift, or slow climate adjustment, is contributing to the decreasing temperatures in the ECHO-G Erik simulation during the 1000–1500 period. The evidence for this is that (i) there is only a small trend in the forcing over that period (the maximum change is only about -0.5 W m^{-2}, from the 12th to 15th centuries, compared with more than $+1.5$ W m^{-2} since 1700), (ii) the MAGICC model is unable to replicate the trend, yet performs well in all other respects, and (iii) the time series of inter-model differences (not shown) slowly levels off near to zero, indicative of a gradual convergence following on from initially different states.

There are two possible sources of drift in the ECHO-G Erik simulation. First, the initial conditions taken in year 901 from the present-day control run may be out of equilibrium with the present-day forcings applied to that run. This would be apparent by drift, or trends, in that control simulation. Inspection of the present-day control run data (not shown here) shows no drift in the global-mean temperature but a downward drift of around -0.2 K in the NH temperature during the overlap period with the Erik simulation. The MAGICC simulation does not include this drift, because the initial conditions used in year 901 were assumed to be in equilibrium with the present-day forcing. Second, the pre-1000 adjustment period, intended to allow the reduction from present-day to pre-industrial forcing conditions, is insufficient to allow the climate to adjust fully to the lower level of forcing. It is not possible to quantify the magnitude of the effect after 1000 because an appropriate simulation with forcing held fixed after 1000 has not been completed with the ECHO-G model (though we understand that early attempts at such an experiment resulted in a cooling trend that extended over a number of centuries—U. Cubasch, personal communication). It is possible to estimate this drift indirectly, however, because such a simulation is easy to do with the tuned MAGICC model, and the results for each variable are indicated by the dashed lines in Fig. 4. The magnitude of this second drift over the period 1000–1990 is indicated by the horizontal lines that mark the simulated values in 1000 and 1990. This drift, according to the MAGICC model, is -0.24 K for global temperature, -0.30 K for NH temperature, and $+0.41$ W m^{-2} for the ocean heat flux.

Without a comparable ECHO-G simulation, it is not possible to test how well MAGICC simulates the drift. Nevertheless, if we assume that ECHO-G would have adjusted to the changed forcing in a similar way (in terms of magnitude and adjustment time scale), then we can use the MAGICC simulation to "correct" the Erik simulation. Subtracting the MAGICC simulation with fixed forcings after 1000 from the main MAGICC simulation gives the same results as when MAGICC was subjected to the same forcing history but started from initial conditions in balance with the forcing in year 1000. Of course, the real climate conditions in the year 1000 are not known, so it is probably incorrect to assume that they were in balance with the forcing; it is likely, however, that they were nearer to equilibrium than the conditions used in ECHO-G, shown clearly by Fig. 4 to be relatively warm. MAGICC could be used to explore sensitivity to a range of reasonable initial conditions, or could be forced from an earlier period (e.g. the whole of the last 2,000 years) to obtain conditions in 1000 that were in accordance with estimates of the earlier forcing, allowing an assessment of the likely degree of disequilibrium in 1000. The aim of the present paper is to compare ECHO-G Erik with other model simulations, however, and the experimental design for most of the other simulations shown in Fig. 2 would have resulted in initial conditions that were near to equilibrium at the start of each run. We choose, therefore, to adjust the Erik simulation by subtracting the MAGICC run with fixed forcings after 1000, because this gives our best estimate of how ECHO-G would have behaved had it started from equilibrium conditions. For the NH temperature, we also subtract the long-term changes in the present-day control run of ECHO-G (approximately -0.2 K over the length of the run), as an additional source of climate drift.

It was noted in Sect. 2 that the ECHO-G Erik simulation did not include all anthropogenic forcings, notably the cooling effect of tropospheric sulphate aerosols. Even though the aerosol forcing is uncertain (Ramaswamy et al. 2001), the central estimate of the direct albedo and indirect cloud property (1st type) forcings is negative and therefore it is likely that the omission of sulphate forcing may contribute to the greater recent warming in ECHO–G Erik than in other simulations which included this forcing (Fig. 2a, b). This possibility was investigated using MAGICC, by modifying the forcing applied to the model (Fig. 1) to

include the central estimate of tropospheric sulphate aerosol forcing used by Wigley and Raper (2002). The forcing is geographically variable, and is specified separately for each of the four boxes—the greatest cooling effect is in the NH, which is clearly important for the comparison shown in Fig. 2. The global-mean of this central estimate reaches -1.1 W m^{-2} in 1990. The forcing was modified further, to include the Wigley and Raper (2002) central estimates of the forcing due to changes in tropospheric and stratospheric ozone and halocarbons too. The total of these additional forcings reaches -0.5 W m^{-2} in the 1990 global-mean. The recent cooling simulated by MAGICC in response to this additional forcing is also applied to the ECHO-G simulation. To do this, a number of assumptions about the similarity of MAGICC and ECHO-G behaviour must be made, but without undertaking an additional ECHO-G run using these forcings, the MAGICC model provides our only available estimate of their effect.

Figure 6 shows the MAGICC and ECHO-G simulated NH temperature after all modifications described above have been made, compared with the original ECHO-G Erik simulation. The adjustment for present-day ECHO-G control run drift has brought the ECHO-G data much closer to the MAGICC run (note that the vertical scale is the same as in Fig. 4b to allow easy comparison). Adjusting the initial conditions to be in equilibrium with the forcing in 1000 (as estimated using MAGICC) lowers the early temperatures in both simulations relative to later temperatures. Much of the warming in recent decades has been removed by the inclusion of the other forcings (i.e. the cooling influence of tropospheric sulphate aerosols), with the difference reaching 0.6 K by the end of the simulation.

7 Comparison of the modified Erik simulation with other simulations

The earlier intercomparison of simulated NH temperatures for the last 1,000 years is revisited in Fig. 2c, with the original ECHO-G Erik time series replaced by the modified data described in Sect. 6 and shown in Fig. 6. The modified simulation no longer appears to be atypical when compared with the other model runs. Some differences remain, of course, but these are expected because of internal climate variability (except in the energy-balance models that do not simulate such variability), differences in the forcings applied to each model (in addition to those investigated here), and differences in each model's global and regional sensitivity to forcing. Though the adjusted temperatures are much lower than the original temperatures in the early centuries, they do remain slightly above the other models for the 1000–1250 mean. This might be related to our use of the simple MAGICC model to estimate the drift/adjustment behaviour of the complex GCM-based ECHO-G model. Finally, note that it is not significant that the 1990 adjusted temperatures are cooler than mid-20th or mid-12th century values, because the recent tropospheric sulphate aerosol forcing is so uncertain (Ramaswamy et al. 2001) that other choices could have been made with equal justification, and could have resulted in adjusted ECHO-G 1990 temperatures lying at either the bottom or the top of the range of other models.

8 Discussion and conclusions

The ECHO-G "Erik" simulation (Gonzalez-Rouco et al. 2003; von Storch et al. 2004) of the climate of the

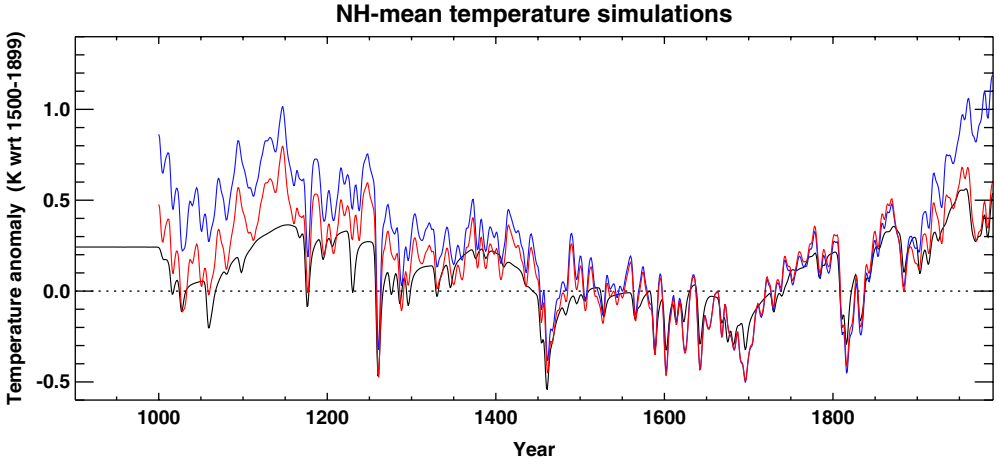

Fig. 6 As Fig. 4b, but after the simulations have been adjusted (i) to remove drift in the present-day control run (ECHO-G only); (ii) to remove drift following the pre-1000 adjustment to lower pre-industrial forcing levels [ECHO-G and MAGICC (Model for the Assessment of Greenhouse-gas-Induced Climate Change)]; and (iii) to include the expected influence of forcings (tropospheric sulphate aerosols, tropospheric and stratospheric ozone, and halocarbons) that were not included in the original Erik experiment (ECHO-G and MAGICC). The Northern Hemisphere temperatures shown are the adjusted MAGICC (*black*), the adjusted ECHO-G (*red*) and the unadjusted ECHO-G (*blue*, repeated from Fig. 4b)

last millennium exhibits quite different behaviour to a set of seven other model simulations, with a much stronger cooling trend during the first 7 centuries and a much stronger warming trend during the final 2 centuries of the millennium (Fig. 2b). The set of simulations used in the comparison were from climate models that varied in complexity from simple energy-balance/ocean-column models to coupled atmosphere–ocean GCMs. It was shown that the visual intercomparison of the simulated NH temperatures is sensitive to the choice of reference period. This choice is arbitrary, of course, but here we prefer to use each simulation's 1500–1899 mean, which is the maximum (pre-20th century) common overlap period of all the simulations.

The MAGICC simple climate model (Wigley and Raper 1992, 2002) is able to replicate the ECHO-G simulation quite closely on various time scales (ranging from the multi-annual response to individual volcanic forcing spikes up to the multi-century response to slowly varying forcing), provided that appropriate parameter values are selected and the initial conditions and forcing history match those used in ECHO-G. The main discrepancy between the ECHO-G and MAGICC simulations is that MAGICC simulates only part of the cooling trend during the first 7 centuries. The climate sensitivity is the most important parameter, and this was set to the central estimate of the effective climate sensitivity that was diagnosed directly from the ECHO-G simulation, equivalent to 2.39 K for a doubling of CO_2. The climate sensitivity for this particular version of ECHO-G has not previously been documented [Goosse et al. (2005) state a value of 3.2 K, but the basis for this is not made clear and it should be treated with caution], though a similar version of the atmospheric GCM coupled to a different ocean model has been reported to have an effective sensitivity of 2.6 K (Cubasch et al. 2001; ECHAM4/OPYC in Table 9.1). The sensitivity diagnosed in this paper has a large uncertainty associated with it (at least 2.28–2.99K), partly because the forcing perturbations applied to this model during the last millennium are relatively small. Nevertheless, when values outside the range 2.3–2.5 K are used in the MAGICC model, the similarity between MAGICC and ECHO-G begins to degenerate.

Experiments with the MAGICC model were then used to demonstrate that the ECHO-G experimental design (using present-day conditions from 901 to 920 followed by a reduction towards pre-industrial forcing), would have led to conditions in 1000 that were probably warmer than appropriate for the pre-industrial forcing. The ongoing adjustment from this initial disequilibrium would then contribute artificially to the simulated cooling trend during the early centuries of the run. For MAGICC, the amplitude of this artificial cooling was 0.3 K for NH temperature over the entire simulation. Examination of the ECHO-G present-day control run from which the experiment was initialised suggests that the NH temperature may have an additional drift of almost 0.2 K cooling per 1,000 years. The ECHO-G simulation has been modified using these estimates of control run drift and ongoing adjustment to the initial forcing reduction. There are two major assumptions involved in making these modifications: first, that the MAGICC model is capable of simulating the response to the initial forcing reduction correctly, and second, that the real climate system was near to equilibrium in year 1000. Though this second assumption is arguable, there is no evidence (Jones and Mann 2004) that forcing prior to 1000 was sufficiently high to have caused conditions in 1000 to be as far from equilibrium as the ECHO-G Erik conditions appear to be.

The ECHO-G Erik simulation included most, but not all, of the most important climate forcings expected to influence the climate during the last 1,000 years. The most significant omission is that no anthropogenic tropospheric sulphate aerosol forcing was included. Though the magnitude of this forcing factor is very uncertain, the likely range of forcing change from 1750 to present is negative (Ramaswamy et al. 2001). Using the tuned MAGICC model, the influence of this missing negative forcing has been quantified for one example choice of the forcing magnitude. The results demonstrate that this forcing might reduce the NH warming during the final century of the millennium by about 0.5 K.

Recently, Goosse et al. (2005) have also investigated differences between the ECHO-G Erik simulation and the simulation with the NCAR CSM model (C.M. Ammann et al., submitted for publication). They noted the possibility that the spin-up procedure (and hence the conditions in 1000) may have contributed to the early warmth in ECHO-G. We have extended their study by using MAGICC to quantitatively assess this problem (Fig. 6). Goosse et al. (2005) also note that the absence of tropospheric sulphate aerosols results in much larger warming in Erik during the last 150 years; again, the present study attempts to quantify the magnitude of this effect (Fig. 6). Goosse et al. (2005) could not separate out this specific influence because their Fig. 3a and Fig. 3b have different implicit "sensitivities" as well as different forcing histories.

Goosse et al. (2005) focus on the likelihood that different climate sensitivity is the major explanation for the difference between the two models' simulations. We have some reservations about the simple scaling of simulations employed by Goosse et al. (2005) to investigate this, because scaling an entire simulation by a constant factor can give a different result to running the experiment with a higher (or lower) sensitivity model. This stems from the fact that the climate response is a *non-linear* function of the climate sensitivity that depends on the time scale of the forcing in such a way that at shorter time scales, the sensitivity has a smaller influence on the response, until at the high frequency limit the response is independent of the sensitivity (Wigley and Raper 1991; Wigley et al. 2005). By scaling the response at all time scales from decadal to millennial

equally, Goosse et al. (2005)'s approach cannot account for this behaviour. The diagnosis of climate sensitivity used here does, however, take this into account because it includes the changing heat content term (F in Eq. 1) that captures the time scale dependence. Subsequently running the MAGICC model with the diagnosed climate sensitivity reproduces the correct behaviour, to the extent that MAGICC is able to capture the time scale dependence of the effective heat capacity of the climate system (Wigley and Raper 1991).

The Goosse et al. (2005) results may also be biased by the artificially strong cooling trend during the early centuries of the ECHO-G Erik simulation. Their scaling factors were determined from the standard deviations of the decadal mean temperatures between 1200 and 1850. The cooling trend during most of this period contributes greatly to this standard deviation for ECHO-G and if, as demonstrated here, this trend is spuriously large, then the scaling factors obtained by Goosse et al. (2005) for ECHO-G will also be too large. Evidence that this may have occurred is given by Fig. 3b of Goosse et al. (2005), which indicates that the recent warming is overestimated by their scaled simulations (though it is not clear by how much because the time series extends beyond the vertical scale of their figure). It is likely, therefore, that Goosse et al. (2005) have overestimated the importance of climate sensitivity for explaining the differences between the ECHO-G and NCAR CSM simulations. We do not discount the contribution of sensitivity differences, but we suggest that it is less important than the contribution from the initial condition and sulphate forcing differences. The effective climate sensitivity diagnosed here takes into account any drift in the early part of the simulation because that appears as a non-zero ocean heat flux (Fig. 4c) term. The value we obtain for ECHO-G, 2.39 K, is only moderately higher than the 2 K equilibrium sensitivity quoted by Goosse et al. (2005) for the NCAR CSM model.

We have been able to adjust the ECHO-G simulation (at hemispheric and global scales) by using the MAGICC simulations to quantify the effects of initial conditions and tropospheric sulphate forcing. These adjustments rely on the assumption that MAGICC is capable of emulating the ECHO-G behaviour, an assumption that has been tested to the extent allowed by the single Erik simulation available to us. When the adjustments are made, the ECHO-G simulation is no longer a clear outlier in the context of the other seven climate model simulations in our comparison (Fig. 2c). Some differences remain between all simulations, and future work (for which MAGICC would again be useful) could quantify the contribution of differences in forcings and model sensitivities, as well as internally generated variability.

The principal finding here is that the amplitude (range) of millennial-scale NH temperature variability simulated in the ECHO-G Erik run may be too strong by around 0.5 K (around 1.5 times too large). This has implications for the conclusions of von Storch et al. (2004), who used this ECHO-G simulation to indicate that centennial climate variability may have been underestimated in empirical climate reconstructions by a factor of 2 or more. Though our results do not discount the bias in climate reconstructions identified by von Storch et al. (2004), which is an inherent property of the reconstruction methods, it is likely that the magnitude of this bias depends on the magnitude of long-term temperature variability (Osborn and Briffa 2004). If the ECHO-G Erik run overestimates this, then the bias in climate reconstructions found by von Storch et al. (2004) will also be overestimated. Note, however, that in this paper we have suggested that the long-term temperature variability is overestimated relative to other climate model simulations, and not necessarily with respect to the evolution of the real climate system. This is a critical distinction, though it is also clear that this ECHO-G simulation should not be used without caveats to support evidence for greater temperature variability in the past [as was done by Moberg et al. (2005), for example].

Acknowledgements This research was supported by the European Community under Research Contract EVK2-CT2002-00160 SOAP. Grateful acknowledgement is given to Eduardo Zorita and Fidel Gonzalez-Rouco for allowing access to the ECHO-G model data, to Julie Jones for providing the data, to Tom Wigley for information about anthropogenic forcing time series, and to two anonymous reviewers for their constructive comments.

References

Bauer E, Claussen M, Brovkin V, Huenerbein A (2003) Assessing climate forcings of the Earth system for the past millennium. Geophys Res Lett 30:1276

Bertrand C, Loutre MF, Crucifix M, Berger A (2002) Climate of the last millennium: a sensitivity study. Tellus A 54:221–244

Crowley TJ (2000) Causes of climate change over the past 1000 years. Science 289:270–277

Crowley TJ, Baum SK, Kim KY, Hegerl GC, Hyde WT (2003) Modeling ocean heat content changes during the last millennium. Geophys Res Lett 30:1932

Cubasch U, Meehl GA, Boer GJ, Stouffer RJ, Dix M, Noda A, Senior CA, Raper S, Yap KS (2001) Projections of future climate change. In: Houghton JT, Ding Y, Griggs DJ, Noguer M, van der Linden PJ, Dai X, Maskell K, Johnson CA (eds) Climate change 2001: the scientific basis (contribution of WG1 to the third assessment report of the IPCC). Cambridge University Press, Cambridge, pp. 525–582

Foukal P, North G, Wigley T (2004) A stellar view on solar variations and climate. Science 306:68–69

Free M, Robock A (1999) Global warming in the context of the little ice age. J Geophys Res 104:19057–19070

Gerber S, Joos F, Brugger P, Stocker TF, Mann ME, Sitch S, Scholze M (2003) Constraining temperature variations over the last millennium by comparing simulated and observed atmospheric CO_2. Clim Dyn 20:281–299

Gonzalez-Rouco F, von Storch H, Zorita E (2003) Deep soil temperature as proxy for surface air-temperature in a coupled model simulation of the last thousand years. Geophys Res Lett 30:2116

Goosse H, Crowley TJ, Zorita E, Ammann CM, Renssen H, Driesschaert E (2005) Modelling the climate of the last millennium: what causes the differences between simulations? Geophys Res Lett 32:L06710

Gregory JM, Ingram WJ, Palmer MA, Jones GS, Stott PA, Thorpe RB, Lowe JA, Johns TC, Williams KD (2004) A new method for diagnosing radiative forcing and climate sensitivity. Geophys Res Lett 31:L03205

Hansen J, Sato M, Ruedy R (1997) Radiative forcing and climate response. J Geophys Res 102:6831–6864

Harvey D, Gregory J, Hoffert M, Jain A, Lal M, Leemans R, Raper S, Wigley T, de Wolde J (1997) An introduction to simple climate models used in the IPCC second assessment report (IPCC technical paper II). IPCC, Geneva, 59 PP

Hirsch RM, Gilroy EJ (1984) Methods of fitting a straight line to data: examples in water resources. Water Resour Bull 20:705–711

Jones PD, Mann ME (2004) Climate over past millennia. Rev Geophys 42:RG2002

Kattenberg A, Giorgi F, Grassl H, Meehl GA, Mitchell JFB, Stouffer RJ, Tokioka T, Weaver AJ, Wigley TML (1996) Climate models—projections of future climate. In: Houghton JT, Meira Filho LG, Callander BA, Harris N, Kattenberg A, Maskell K (eds) Climate change 1995: the science of climate change (contribution of WG1 to the second assessment report of the IPCC). Cambridge University Press, Cambridge, pp. 285–357

Kheshgi HS, Jain AK (2003) Projecting future climate change: implications of carbon cycle model intercomparisons. Global Biogeochem Cycles 17:1047

Lean J, Beer J, Bradley R (1995) Reconstructions of solar irradiance since 1610—implications for climate change. Geophys Res Lett 22:3195–3198

Legutke S, Voss R (1999) ECHO-G, the Hamburg atmosphere-ocean coupled circulation model. DKRZ technical report, 18, DKRZ, Hamburg

Mann ME, Jones PD (2003) Global surface temperatures over the past two millennia. Geophys Res Lett 30:1820

Mann ME, Rutherford S, Wahl E, Ammann C (2005) Testing the fidelity of methods used in proxy-based reconstructions of past climate. J Clim 18:4097–4107

Moberg A, Sonechkin DM, Holmgren K, Datsenko NM, Karlen W (2005) Highly variable Northern Hemisphere temperatures reconstructed from low- and high-resolution proxy data. Nature 433:613–617

Murphy JM (1995) Transient-response of the Hadley Center coupled ocean-atmosphere model to increasing carbon-dioxide. 3. Analysis of global-mean response using simple-models. J Clim 8:496–514

Osborn TJ, Briffa KR (2004) The real color of climate change? Science 306:621–622

Ramaswamy V, Boucher O, Haigh J, Hauglustaine D, Haywood J, Myhre G, Nakajima T, Shi GY, Solomon S (2001) Radiative forcing of climate change. In: Houghton JT, Ding Y, Griggs DJ, Noguer M, van der Linden PJ, Dai X, Maskell K, Johnson CA (eds) Climate change 2001: the scientific basis (contribution of WG1 to the third assessment report of the IPCC). Cambridge University Press, Cambridge, pp. 349–416

Raper SCB (2004) Interpretation of model results that show changes in the effective climate sensitivity with time. Workshop on climate sensitivity, Paris, France, 26–29 July 2004. IPCC working group 1 technical support unit, Boulder, pp. 131–133

Raper SCB, Cubasch U (1996) Emulation of the results from a coupled general circulation model using a simple climate model. Geophys Res Lett 23:1107–1110

Raper SCB, Gregory JM, Osborn TJ (2001) Use of an upwelling-diffusion energy balance climate model to simulate and diagnose A/OGCM results. Clim Dyn 17:601–613

von Storch H, Zorita E, Jones JM, Dimitriev Y, Gonzalez-Rouco F, Tett SFB (2004) Reconstructing past climate from noisy data. Science 306:679–682

Widmann M, Tett SFB (2003) Simulating the climate of the last millennium. PAGES Newsletter 11(2/3):21–23

Wigley TML, Raper SCB (1991) Internally generated natural variability of global-mean temperatures. In: Schlesinger M (ed) Greenhouse-gas-induced climatic change: a critical appraisal of simulations and observations. Elsevier Science Publishers, Amsterdam, pp. 471–482

Wigley TML, Raper SCB (1992) Implications for climate and sea-level of revised IPCC emissions scenarios. Nature 357:293–300

Wigley TML, Raper SCB (2001) Interpretation of high projections for global-mean warming. Science 293:451–454

Wigley TML, Raper SCB (2002) Reasons for larger warming projections in the IPCC third assessment report. J Clim 15:2945–2952

Wigley TML, Ammann CM, Santer BD, Raper SCB (2005) Effect of climate sensitivity on the response to volcanic forcing. J Geophys Res 110:D09107

Yohe G, Andronova N, Schlesinger M (2004) Climate—to hedge or not against an uncertain climate. Science 306:416–417

Zorita E, Gonzalez-Rouco F, Legutke S (2003) Testing the Mann et al. (1998) approach to paleoclimate reconstructions in the context of a 1000-yr control simulation with the ECHO-G coupled climate model. J Clim 16:1378–1390